

# Multi-response Optimization of Process Parameters of TIG Welding for Dissimilar Metals (SS-304 and Fe-410) using Grey Relational Analysis

Ashishkumar Wahule<sup>1</sup>, Prof. Kushal Wasankar<sup>2</sup>

<sup>1</sup>PG Student, Mechanical Engineering Department, Government College of Engineering, Aurangabad (M.S), India

<sup>2</sup> Assistant Professor, Mechanical Engineering Department, Government College of Engineering, Aurangabad (M.S), India

\*\*\*

**Abstract** - The aim of this research work is to weld the dissimilar metals, stainless steel and mild steel (SS-304 and Fe-410). Joining of mild steel and stainless steel finds wide applications in chemical, oil and petroleum industry in the fabrication of pressure vessels and the storage tanks. But the joining of dissimilar metals is a major challenge as the amount of contamination in the weld area is very high which affects the weld properties. TIG welding process is generally applied to the wide range of metals which uses non consumable tungsten electrode. The tensile strength and the percentage elongation of the welded joint should be higher. The various process parameters selected for joining the metals affect the mechanical properties of the welded joint. Hence, to find out the optimum values of the tensile strength and the percentage of elongation is the main objective of this research work. Grey Relational Analysis is used to optimize the multiple responses simultaneously.

**Key Words:** TIG welding, Mild Steel, Stainless Steel, Multi-response optimization.

## 1. INTRODUCTION

Welding is the manufacturing process generally used for joining metal parts. Welding is used for joining the metals when the lengths of standard sections are more or to fabricate the desired structure by joining the different parts together. TIG welding process is commonly used for joining of two similar or dissimilar metals which uses a non-consumable tungsten electrode for producing the arc and an inert gas or mixture of gases to protect the weld contamination. TIG welding is also popularly known as Gas Tungsten Arc Welding (GTAW). TIG welding finds its application in joining of mild steel and stainless steel pipes as well as sheets of different thickness and standard dimensions. Pressure and filler wire may or may not be used in the TIG welding process. The stainless steel and mild steel dissimilar metal joints are very common structural applications and the joining of these metals is very critical as carbon precipitation and chromium loss leads to increase in porosity and affects the strength of the joint [1]. The quality of the weld is mainly dependent on bead geometry features, metallurgical and mechanical characteristics and various aspects of weld chemistry [3]. The output welding properties are extensively influenced by input parameters like current, voltage, gas flow rate, filler rod material, weld position and the welding speed.

By varying the combination of input process parameters, the output properties obtained would be different for the welded joints. The arc welding is generally characterized as a multiple-input, multiple-output system.

## 1.1 TIG Welding Operation

TIG welding is an arc welding process. Wherein coalescence is produced by heating the work piece with an electrical arc struck between a tungsten electrode and the job. The electrical discharge generates a plasma arc between the electrode tip and the work piece to be welded. The arc is normally initialized by a power source with a high frequency generator. This produces a small spark that provides the initial conducting path through the air for the low voltage welding current. The arc generates high-temperature generally about 6100 °C and melts the surface of base metal to form a molten pool. To avoid atmospheric contamination of the molten weld pool a welding gas (argon, helium, nitrogen etc) is used. As the molten metal cools, coalescence occurs and the parts are joined. The obtained weld is smooth and requires minimal finish [13]. To obtain the optimum values of the desired mechanical properties it is important to select the proper levels of the input parameters. The input parameters selected are current, gas flow rate and the root gap. While the output responses analyzed are tensile strength and % elongation by using Grey Relational Analysis.

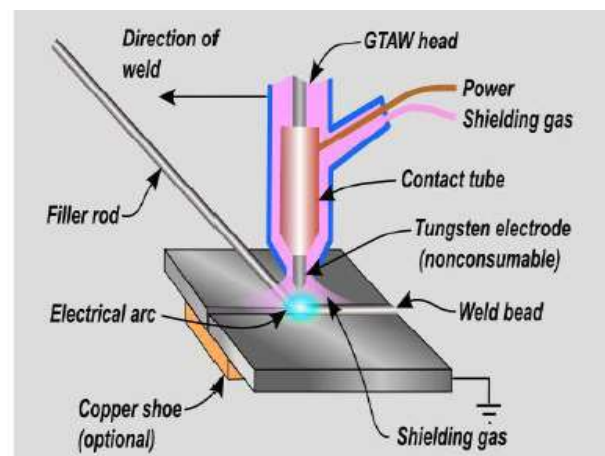


Fig-1: TIG welding set-up

## 2. LITERATURE REVIEW

Radha Mishra et al, [5] investigated the tensile strength of MIG and TIG welded dissimilar joints of mild steel and stainless steel. TIG and MIG welding process were used for welding different grades of steel with mild steel. Four test samples were prepared by welding SS202, SS304, SS310 and SS316 with mild steel. It was found that TIG is more suitable than MIG for dissimilar metal welding of mild steel and stainless steel as it provides better strength. Also, the dilution percentage in stainless steel is found to be higher in MIG welded dissimilar joints.

Lokesh Kumar G, et al. [6] studied some fundamental observations on the microstructure and the mechanical properties, formed by AISI 304 (ASS) and AISI 430 (FSS) with AWS E308L austenitic stainless steel covered electrode. Thus, forming a dissimilar weld joint with the use of filler material. The welding processes carried out in the experiment are shielded metal arc welding (SMAW) and tungsten inert gas welding (TIG). The results obtained were analyzed for welding processes of dissimilar welded joints of stainless steel. From the results obtained it was concluded that the better tensile strength is obtained from TIG process when it is compared to SMAW process.

Madduru Phanindra Reddy, et al. [7] in this study bimetallic joint of low alloys and stainless steel commonly used in high temperature corrosion environments applications are formed using TIG welding. In this investigation, attempts have been made to investigate the weldability of AISI 4140 and AISI 316 by TIG welding process with and without using filler metal. For joining this dissimilar metals ER 309L was used as filler material. Hardness and tensile strength are the properties considered for the study.

Vikas Chauhan, et al. [8] studied the parametric optimization of MIG welding for stainless steel (SS-304) and low carbon steel using Taguchi design method. Three parameters of MIG welding viz. current, voltage and travel speed are taken for the analysis. A plan of experiments based on Taguchi technique has been used to acquire the data. MIG welding process is very successful to join stainless steel (SS-304) and low carbon steel. Taguchi method is used to discover the influence of process parameters (current, voltage and welding speed) on the ultimate tensile strength.

Cheng-Hsien Kuo et al, [9] studied the effect of TIG flux on the performance of dissimilar welds between mild steel G3131 and stainless steel 316L. The experiments were conducted to investigate the effect of CaO, Fe<sub>2</sub>O<sub>3</sub>, Cr<sub>2</sub>O<sub>3</sub> and SiO<sub>2</sub>. The surface appearance of TIG welds produced with oxide flux tended to form the residual slag. Improvements in joint penetration and increased weld depth to width ratio were obtained by using SiO<sub>2</sub> powder.

## 3. EXPERIMENTAL DETAILS

### 3.1 Raw Material

The raw material consists of both consumable filler material as well as the non-consumable tungsten electrode. The joining of dissimilar metals is done in many industries. The pressure vessels, storage tanks and their support systems are fabricated using the dissimilar metals in order to reduce the fabrication cost. For the experimentation, 9 MS plates and 9 SS plates of dimensions 100\*50\*6 are prepared as shown in figure 2.

According to DOE technique, 9 plates of MS and plates of SS are required to form L9 orthogonal array design. Figure 2 shows the plates used for welding.



Fig-2: Raw material

Selection of filler material is very important for joining of the dissimilar metals. Generally, low carbon stainless steel filler material is used for joining dissimilar metals. In order to prevent the welding contamination, oxides on the surface of filler and work piece should be removed and immediately prior to welding acetone or alcohol should be used to clean the surface. The chemical composition of SS-304 and Fe-410 is as shown in tables below.

The chemical conformation of the material was done at S. N. Metallurgy, Aurangabad. The SS-309L is used as the filler material for joining of the material and the argon gas is used for the shielding purpose.

Table-1: Chemical composition of SS-304

SS-304		
Chemical Composition	%C	0.032
	%Mn	1.28
	%S	0.006
	%P	0.013
	%Si	0.42
	%Ni	8.20

**Table-2:** Chemical composition of Fe-410

Fe-410		
<b>Chemical Composition</b>	%C	0.17
	%Mn	0.66
	%S	0.020
	%P	0.019
	%Si	0.20
	%Ni	0.03

**3.2 Test Procedure**

By using the star protector the bevel angle of 60° was made. Root face of 1 mm was also provided on each side of the plate. The input parameters were selected as per the L9 orthogonal array. After joining the plates, the weld bead was cleaned using cloth and acetone.

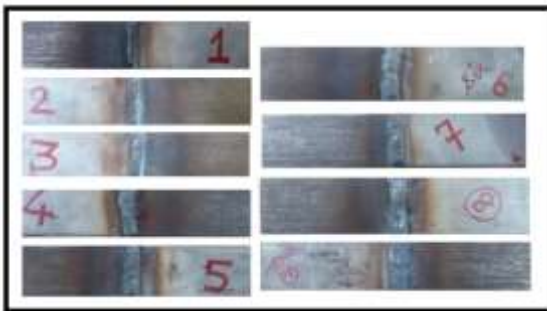


**Fig-3:** Welded samples

**3.3 Machining of welded samples for testing**

The welded samples were welded as per the ASTM standards and the outer portions were cut to remove the discontinuities.

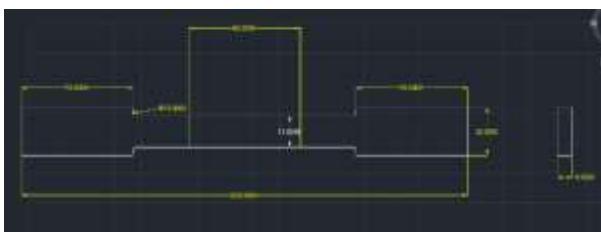


**Fig-4:** AUTO-CAD model of samples to be machined

The samples were prepared for the testing by using the parameters from the orthogonal array. The samples were machined as per the ASTM section IX.

**3.4 ASTM Standards for Tensile Testing**

The welded specimens are machined as per the ASTM standards with dimensions 200\*50\*6 mm and are

used for testing. The two third of the grip sections are loaded in the UTM.

**Table-3:** ASTM Dimensions for Tensile Test

Gauge Length	50 mm
Width of reduced Section	13mm
Radius of the fillet	13mm
Overall length	200mm
Length of the reduced section	60mm
Length of the grip section	50mm

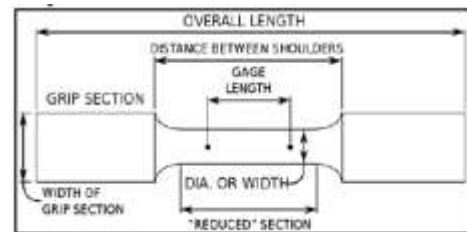


**Fig-5:** ASTM Dimensions

Table 3 shows the values of process parameters at three levels and table 4 shows L9 orthogonal array.

**Table-4:** Process parameters and their values

Input Parameters	Levels of Parameters		
	Level 1	Level 2	Level 3
Current (Amp)	80	100	120
Gas Flow Rate (lit/min)	08	12	16
Root Gap (mm)	0	1	2

**Table-5:** Taguchi L9 orthogonal array

Sr. No.	Current	Gas Rate	Flow	Root Gap
1	80	08		0
2	80	12		1
3	80	16		2
4	100	08		1
5	100	12		2
6	100	16		0
7	120	08		2
8	120	12		0
9	120	16		1

The samples are machined as per the ASTM standards and are used for the testing purpose. The machined samples are as shown in figure 6.



**Fig-6:** Machined Samples

**4. RESULTS AND DISCUSSION**

**4.1 Results and Analysis for Ultimate Tensile Strength (UTS)**

The results of the tensile tests are as shown in the table 6 below.

**Table-6:** Ultimate tensile strength

Sample Number	Calculated UTS (MPa)
1	292
2	297
3	321
4	290
5	310
6	328
7	336
8	318
9	343

For the evaluation of the optimum results software MINITAB 17 was used in this experimentation work. Table 6 represents calculated tensile strength from the observed load. In this software the means plot is plotted with the calculations of the S/N ratio. The following are results obtained from MINITAB 17. The broken samples are shown in the figure 7.



**Fig-7:** Samples after tensile test

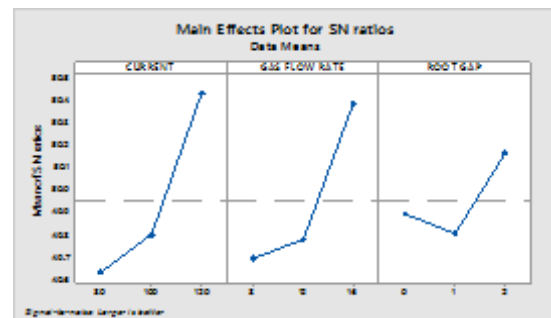


**Chart-1:** Means Plot for Tensile Test

The ANOVA Calculation of the ultimate tensile strength was performed in Excel Software. Sum of Squares and mean square readings are calculated. From these readings the F ratio and % Contribution of F are observed as shown in table 7.

**Table-7:** ANOVA calculations for UTS

Source	DF	Sum of Sq.	Mean of Sq.	F	% Contribution
Current	2	1.0578	0.5289	8.32	47.38
GFR	2	0.8527	0.4262	6.71	37.95
RG	2	0.2006	0.1046	1.65	8.92
Residual Error	2	0.1271	0.06353		5.65
Total	8	2.2466			

From the ANOVA calculations it is found that percentage of contribution of current is maximum for the UTS which is about 47.38% followed by gas flow rate(37.95%) and root gap(8.92%).

#### 4.2 Results and analysis for Percentage Elongation

The gauge length of 50 mm was marked on the specimen and the amount of elongation in the gauge length was calculated using vernier caliper.

**Table-8:** Percentage Elongation

Sample Number	Percentage Elongation ( % )
1	10
2	10
3	12
4	12
5	10
6	12
7	20
8	12
9	22

For the evaluation of the optimum results software MINITAB 17 was used in this experimentation work. Table 7 represents calculated percentage elongation from the samples. In this software the means plot is plotted with the calculations of the S/N ratio. The following are results obtained from MINITAB 17. Figure 9 and 10 represents the window of MINITAB 17 software for means plot.

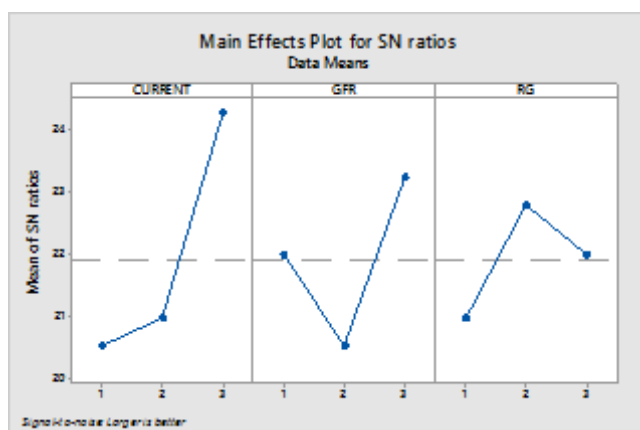


**Chart-2:** Means Effects Plot for Percentage Elongation

The ANOVA calculation of the percentage elongation was performed in Excel Software as shown in table 9. Sum of Squares and mean square readings are calculated. From these readings the F ratio and % Contribution of F are observed.

**Table-9:** ANOVA for Percentage Elongation

Source	DF	Sum of Sq.	Mean of Sq.	F	%
Current	2	32.8313	16.4156	22.53	62.88
GFR	2	12.5737	6.2868	8.63	24.08
RG	2	5.3436	2.6717	3.67	10.23
Residual	2	1.457	0.7285		2.79
Total	8	52.205			

#### 4.3. GRA for Multi Objective Optimization

The GRA is one of the powerful and effective soft tool used to analyze various processes having multiple performance characteristics. GRA is carried out for solving complicated problems which have interrelationships among the designated performance characteristics. The purpose of grey relational analysis the multi-objective problem has been converted into single objective optimization using GRA technique.

Normalize the measured values of UTS and Percentage elongation ranging from zero to one. This process is called as Grey Relational normalization. If the target value of original sequence is infinite, then it has a characteristic of “the larger the better” than the original sequence can be normalized as follows:

$$xi(k) = \frac{yi(k) - \min yi(k)}{\max yi(k) - \min yi(k)} \quad (1.1)$$

If the expectancy is “the smaller the better” than the original sequence should be normalized as follows:

$$xi(k) = \frac{\max yi(k) - yi(k)}{\max yi(k) - \min yi(k)} \quad (1.2)$$

Following data pre-processing, a grey relational coefficient is calculated to express the relationship between the ideal and actual normalized experimental results. The Grey relation coefficient can be express as follows:

$$\zeta i(k) = \frac{\Delta \min + \psi \Delta \max}{\Delta oi(k) + \psi \Delta \max} \quad (1.3)$$

In Grey relation analysis, the grey relation grade is used to show the relationship among the sequences. The Grey Relation grade also indicates the degree of influence that the comparability sequence could exert over the reference sequence. In this study, the importance of both the comparability sequence and reference sequence is treated as equal. Tables 9, 10 & 11 represent the calculations of the GRC and GRG.

**Table-10:** S/N Ratios of Measured Values

Expt. No.	Measured Values		S/N Ratios	
	UTS	% EL	UTS	% EL
1	292	10	49.3077	20.0000
2	297	10	49.4551	21.5836
3	321	12	50.1301	21.5836
4	290	12	49.2480	21.5836
5	310	10	49.8272	20.0000
6	328	12	50.3175	21.5836
7	336	20	50.5268	26.0206
8	318	12	50.0485	21.5836
9	343	22	50.7059	26.8485

**Table-12:** GRC and GRG

Expt. No.	Grey Relational Co-efficient		Grey Relational Grade	Order
	UTS	% EL		
1	0.3419	0.3333	0.3376	9
2	0.3654	0.3333	0.3493	8
3	0.5436	0.3750	0.4593	4
4	0.3333	0.3750	0.3541	7
5	0.4453	0.3333	0.3893	6
6	0.6384	0.3750	0.5067	3
7	0.7910	0.7499	0.7704	2
8	0.5145	0.3750	0.4447	5
9	1	1	1	1

**Table-11:** Normalized values of responses

Expt. No.	Normalized values of UTS and Percentage Elongation	
	UTS	% EL
1	0.0337	0
2	0.1320	0
3	0.5849	0.1667
4	0	0.1667
5	0.3773	0
6	0.7169	0.1667
7	0.8679	0.8333
8	0.5283	0.1667
9	1	1

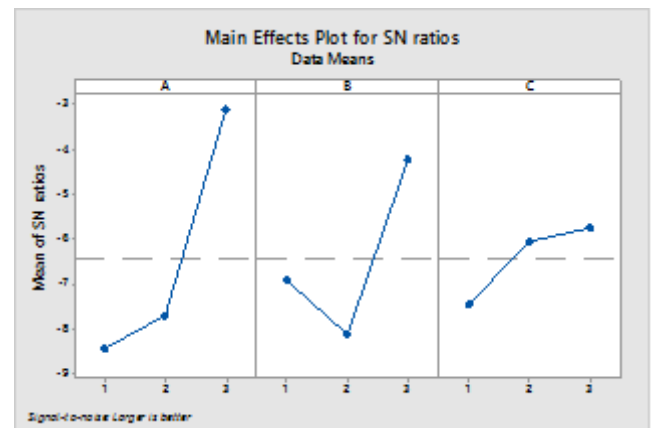


**Chart-3:** Means Effects Plot for Multi-response Optimization

**Table-13:** ANOVA for Multi Objective Optimization

Source	DF	Sum of Sq.	Mean of Sq.	F	%
Current	2	50.262	25.131	7.89	58.73
GFR	2	23.913	11.956	3.75	27.94
RG	2	7.033	2.517	0.79	8.21
Residual	2	4.373	3.186		5.10
Total	8	85.581			

In grey relational analysis total performance of multi objective optimization is depending on value of grey relational grade. According to performed experiment design, it is clearly observed from Table 11 that the TIG Welding process parameters setting of experiment no.9 has the highest grey relation grade. Thus, the 9th experiment gives the best multi-performance characteristics among the 9 experiments. To find out optimum process parameter main effect plot is plotted by using MINITAB-17 as shown in figure 10.

### 5. CONFIRMATION TEST

The regression equations of tensile test and the percentage of elongation are obtained using MINITAB-17.

$$\text{UTS (MPa)} = 200.7 + 0.725 \text{ Current} + 3.08 \text{ Gas Flow Rate} + 4.83 \text{ Root Gap}$$

$$\% \text{ Elongation} = -8.33 + 0.1833 \text{ Current} + 0.167 \text{ Gas Flow Rate} + 1.33 \text{ Root Gap}$$

Table 13 shows the results obtained from the confirmation test.

**Table-14:** Confirmation Test for Tensile Test and % Elongation

Test	Predicted Value	Experimental Value	Error
UTS (MPa)	346.64	344.17	0.7%
% Elongation	17.66	16.48	6.68%

## 6. CONCLUSIONS

The results are obtained for both tensile test as well as percentage elongation. Optimum values for both the tensile test as well as percentage elongation are obtained. The conclusions obtained from the test results are as follows:

- The optimum values for tensile strength was observed as 120 Amps of current, 16 Lit/min of gas flow rate and 2 mm of root gap.
- From the ANOVA, the maximum contribution was found of current i.e. 47.38% followed by gas flow rate i.e. 37.95% and root gap.
- The optimum values for percentage elongation found out as 120 Amp of current, 16 Lit/min, of gas flow rate and 1 mm of root gap.
- From the ANOVA, the maximum contribution was found of current i.e. 62.88% followed by gas flow rate i.e. 24.08% and root gap.
- For multi-objective optimization of tensile strength and percentage elongation, optimum values were found out to be 120 Amps of current, 16 Lit/min of gas flow rate and 2 mm of root gap.
- From the ANOVA, the maximum contribution was found of Current i.e. 58.73 % followed gas flow rate by i.e. 27.94 % and root gap.

## REFERENCES

- [1] Miller, "TIG Welding Handbook", 2013 Miller Electric Mfg. Co. 2013, pp 215-944.
- [2] B. S. Raghuwanshi, "A Course in Workshop Technology", Dhanpat Rai Publications Co., Edition 2008, pp 23-94.
- [3] Phadke M. S., "Quality Engineering Using Robust Design", Prentice Hall International Inc. Englewood Cliffs, NJ, 1989, pp 1-80.
- [4] ASTM Standard A-370, Standard Testing Methods and Definitions for Mechanical Testing of Steel Products.
- [5] R. R. Mishra et al, "A study of tensile strength of MIG and TIG welded dissimilar joints of mild steel and stainless steel," IJAMSE, vol.-3, pp. 23-32, April-2014.
- [6] Lokesh Kumar G, Karthikeyan."Microstructure and mechanical properties of ASS (304) and FSS (430) dissimilar joints in SMAW & GTAW process, IJESRT, 4(6): June, 2015.
- [7] Madduru Phanindra Reddy" Assessment of Mechanical Properties of AISI 4140 and AISI 316 dissimilar weldments" 7th international conference on materials for advance technology, Elsevier, 2014.
- [8] Vikas Chauhan, Dr. R. S. Jadoun and Ankur Singh Bist, "Parametric optimization of MIG welding for stainless steel and low carbon steel using Taguchi design method)", International journal of engineering sciences & research technology, July (2014), 3(7), pp.- 614-620.
- [9] Cheng-Hsien Kuo et al, "Effect of activated TIG flux on performance of dissimilar welds between mild steel and stainless steel," Key Engineering Materials, vol.-479, pp. 74-80, April-2011.
- [10] J. Pasupathy et al, "Parametric optimization of TIG welding parameters using Taguchi method for dissimilar joint," IJSER, vol.-4, pp. 25-28, November-2013.
- [11] R. Rudrapati et al, "Design optimization of process parameters of TIG welding based on Taguchi method," IJCET, vol.-1, pp. 12-16, February-2014.
- [12] S. R. Patil et al, "Optimization of MIG welding parameters for improving strength of welded joints," IJAERS, vol.-2, pp. 14-6, September-2013.
- [13] Jun Yan et al, "Study on micro-structure and mechanical properties of stainless steel joints by TIG, laser and laser-TIG hybrid welding," ELSEVIER, vol.-1, pp. 512-517, September-2009.
- [14] C. N. Patel et al, "Parametric optimization of weld strength of MIG welding and TIG welding by using ANOVA and Grey Relational Analysis," IJRME&ET, vol.-1, pp. 48-56, April-2013.
- [15] A. Prakash et al, "Parametric optimization of TIG welding using Taguchi approach," IJIRSET, vol.-5, pp. 3630-3638, March-2016.
- [16] M. Singla, "Parametric optimization of gas metal arc welding process by using factorial design approach," JMMCE, vol.-9, pp. 353-363, 2010.

- [17] V. Anand Rao et al, "Experimental investigation for welding aspects of stainless steel 310 for process of TIG welding," ELSEVIER, vol.-1, pp. 902-908, 2014.
- [18] P. Giridharan et al, "Optimization of pulsed GTA welding process parameters for welding of AISI304L stainless steel," IJAMT, vol.-1, pp. 478-489, February-2008.
- [19] B. Patel et al, "Optimizing and analysis of parameter for pipe welding: A literature review," IJERT, vol.-2, pp. 229-233, October-2013.
- [20] N. Patel et al, "A review on Optimization of TIG welding," IJCER, vol.-04, pp. 27-31, January-2014.
- [21] A. Singh et al, "Techniques to improve weld penetration in TIG welding (A Review)," ICMPC, vol.-1, pp. 1252-1259, 2017.
- [22] D. Ananthapadmanaban et al, "A study of mechanical properties of friction welded mild steel to stainless steel joints," ELSEVIER, pp. 2642-2646, November-2008.
- [23] R. Sathish et al, "Weldability and process parameter optimization of dissimilar pipe joints using GTAW," IJERA, vol.-2, pp. 2525-2530, June-2012.